

# We are IntechOpen, the world's leading publisher of Open Access books Built by scientists, for scientists

6,900

Open access books available

186,000

International authors and editors

200M

Downloads

Our authors are among the

154

Countries delivered to

TOP 1%

most cited scientists

12.2%

Contributors from top 500 universities



WEB OF SCIENCE™

Selection of our books indexed in the Book Citation Index  
in Web of Science™ Core Collection (BKCI)

Interested in publishing with us?  
Contact [book.department@intechopen.com](mailto:book.department@intechopen.com)

Numbers displayed above are based on latest data collected.  
For more information visit [www.intechopen.com](http://www.intechopen.com)



# Selective Growth of Carbon Nanotubes, and Their Applications to Transparent Conductive Plastic Sheets and Optical Filters

Yusuke Taki, Makiko Kikuchi, Kiyoaki Shinohara,  
Yosuke Inokuchi and Youhei Takahashi

*Smart Materials Research Section, Materials & Advanced Research Laboratory,  
Research & Development Headquarters, Core Technology Center, Nikon Corporation  
Japan*

## 1. Introduction

Carbon nanotubes (CNTs) have incomparable physical properties and their applications in various fields have been examined. In particular, CNTs composed of a few cylindrical walls are useful for optoelectronic applications. The electronic properties of CNTs, however, significantly change depending on their chirality and the number of graphene walls. Therefore, first of all, the selective growth of graphene walls is required, and ultimately, chiral selection technology should be established. In single-walled CNTs (SWCNTs) and double-walled CNTs (DWCNTs), both semiconducting and metallic characteristics exist according to the chirality of the CNTs. On the other hand, it was predicted that all triple-walled CNTs (TWCNTs) have semimetal characteristics. Therefore, TWCNTs may be used in electronic applications without the need for chiral selection. Moreover, because TWCNTs is the finest multi-walled CNTs (MWCNTs), it is academically interesting to clarify the formation mechanism and various properties of TWCNTs.

Nowadays, as-grown SWCNT films are well synthesized on substrates by several types of chemical vapor deposition (CVD) (Hata et al., 2004; Murakami et al., 2004; Zhong et al., 2005). In addition, a synthetic process of producing high-purity SWCNT powder was established at the end of the last century (Nikolaev et al., 1999). As-grown DWCNT films on substrates have also been reported (Hiramatsu et al., 2005; Yamada et al., 2006). From the viewpoint of obtaining DWCNT powder, the CVD of DWCNT powder with supporting material was reported (Muramatsu et al., 2005). The combustion removal of SWCNTs from a mixture of SWCNTs and DWCNTs was also reported (Ramesh et al., 2006). The combustion removal method required a post-treatment to obtain high-yield DWCNT powder. On the other hand, the synthesis of TWCNTs has not reported at all, regardless of the form, for example, films and powder. For the purpose of obtaining CNT films with high DWCNT and TWCNT contents, post-treatments after CNT synthesis are not suitable, because CNTs have almost same chemical properties not related to the number of graphene walls. Post-treatments are only effective for removing amorphous carbon and metallic catalysts from CNTs. Therefore, it is necessary to develop an as-grown synthetic process for DWCNT and TWCNT films.

It is necessary to prevent the aggregation of catalyst particles on a substrate and to control the catalyst diameter distribution on the substrate for the entire period from catalyst deposition to the beginning of CNT growth, because catalyst particles are considered to function as growth nuclei for CNTs. It is necessary for DWCNT and TWCNT syntheses to enlarge the average diameters of catalyst particles more than SWCNT synthesis and to maintain narrow catalyst diameter distributions. In the techniques reported thus far, when catalyst particles are deposited on substrates, catalyst diameter distributions are narrow. While temperature rises slowly up to the CNT growth temperature, the catalyst diameter distributions broaden because of aggregation. As a result, CNTs that consist of various numbers of graphene walls are synthesized involuntarily.

In Section 2.1, it is explained about radiation-heated CVD (RHCVD), which enables us to selectively synthesize SWCNT, DWCNT, and TWCNT films on substrates (Taki et al., 2008a). The number of graphene walls of CNTs has a close relationship to catalyst diameter. It is very important to maintain narrow catalyst diameter distributions for a selective growth of graphene walls. RHCVD is characterized by its use of IR radiation, which enables the entire reactor to be heated rapidly. Therefore, RHCVD has the capability of maintaining narrow catalyst diameter distributions for the entire period from catalyst deposition to the beginning of CNT growth. The principle of RHCVD is explained as follows. First, catalyst particles whose diameters are several nanometers are deposited onto a substrate. Second, an entire reactor in hydrogen atmosphere is heated using IR radiation with an originally developed heating procedure. Catalyst particles should be reduced at a relatively low temperature to prevent their aggregation. Third, after reduction, the reactor is rapidly heated up to a prescribed temperature. During this period, it is considered that alloy particles are created within a narrow diameter distribution. Fourth, hydrocarbon gas is introduced into the reactor. The gas adheres to the catalyst particles, hydrogen is dissociated, and CNTs grow from the catalyst particles. Most of CNTs grown are composed of the same number of graphene walls because the catalyst diameter distribution is controlled within a narrow range.

In addition, in Section 2.2, it is mentioned about the synthesis of vertically aligned SWCNT, DWCNT, and TWCNT films on substrates by a combination of RHCVD and long-throw sputtering as a catalyst particle deposition process (Taki et al., 2008b). For obtaining vertically aligned SWCNT, DWCNT, and TWCNT films, it is necessary to deposit catalyst particles on substrates uniformly with a high population density, prior to RHCVD. When the population density of catalysts on substrates is very high, particles aggregate and the selective growth of graphene walls becomes impossible. In contrast, when the population density is very low, SWCNTs, DWCNTs, and TWCNTs do not grow vertically. In order to solve this dilemma, it is very effective to first deposit non-catalyst particles on a substrate, and secondarily deposit catalyst particles onto non-catalyst particles on the substrates. The diameters of non-catalyst particles must be slightly larger than those of catalyst particles. Even though the population density of catalyst particles on the substrate is quite high, catalyst particles may not aggregate each other during pre-heating process. Because each catalyst particle is located on each non-catalyst particle, a catalyst particle is not able to aggregate with a nearest catalyst particle on another non-catalyst particle.

Section 2.3 explains the essence of synthesizing long CNTs on substrates. It is necessary to delay the inactivation of metallic particles during a CNT growth period. Using Al particles as a non-catalyst, and lowering growth temperature are effective for delaying the inactivation of metallic catalysts.

Transparent conductive plastic sheets containing CNTs have also been studied by some groups. The plastic sheets reported so far have isotropic conductivity (Dan et al., 2009; Hecht et al., 2009; Wu et al., 2004). In contrast, anisotropic conductivity has been achieved in this study. In Section 3, it is explained how to fabricate an anisotropically conductive sheet and comparative study of electrical features using several kinds of CNTs. Anisotropically conductive and transparent plastic sheet is expected for both optical and electronic new applications.

In Section 4, the excellent optical performance of CNT forests is explained in detail. In the field of laser optics, stray light is significant matter to be solved. For example, the reflection on an inner wall of a laser device box induces stray light problem and causes an optical sensor in the box not to work well. Therefore, extremely low-reflection optical elements with a wide incident angle range are necessary for solving stray light. CNT forests, which grow vertically on substrates with a high population density, are effective for such optical applications. By using CNT forests, extremely low-reflection absorbance and ND filter were fabricated and characterized for high power ArF excimer laser equipment.

## 2. CNT growth

### 2.1 Selective growth of SWCNTs, DWCNTs, and TWCNTs through precise control of catalyst diameter by radiation-heated chemical vapor deposition

Dip solutions were prepared by dissolving both  $\text{Co}(\text{CH}_3\text{COO})_2 \cdot 4\text{H}_2\text{O}$  and  $(\text{Mo}(\text{CH}_3\text{COO})_2)_2$  in ethanol. The Co and Mo concentrations in the dip solutions were accurately adjusted to 0.01, 0.02, 0.03, 0.04, 0.05, 0.06, 0.07, 0.08, 0.09, and 0.10 wt%. The Co / Mo mole ratio was maintained at 1/1 for each dip solution. Quartz glass substrates were cleaned ultrasonically, and then hydrophilically modified by UV irradiation in ambient atmosphere. Hydrophilically modified substrates were dipped in the Co / Mo solutions and pulled up at a regular speed. Catalyst diameters on the substrates were controlled by changing the concentrations of the dip solutions. Several substrates which were dip-coated with each concentration were simultaneously placed on a quartz glass holder in a RHCVD reactor. The holder temperature was controlled with a thermocouple and a proportional-integral-derivative controller. The RHCVD reactor was heated up and kept at an intermediate temperature in air. The dip-coated films on the substrates were oxidized and volatile gases were exhausted from the films. After this period, the reactor was evacuated and filled with hydrogen gas at the same temperature. The dip-coated films were reduced and they became metallic particles. The intermediate temperature was as low as the temperature at which catalyst particles scarcely aggregate, and as high as the temperature at which oxidation and reduction reactions progress sufficiently. After that, the reactor was rapidly heated up to 800°C in hydrogen atmosphere. As soon as the temperature reached 800°C, ethanol vapor diluted with argon gas was introduced into the reactor. CNTs grew from the metallic catalyst particles on the substrates. During a CNT growth period of 1 h, the substrate temperature and total pressure were kept at 800°C and 1.7 kPa, respectively.

The characteristics of catalyst particles and the morphology of as-grown CNT films on substrates were observed by scanning electron microscopy (SEM). Two hundred CNTs scratched from each film were observed by transmission electron microscopy (TEM) in order to evaluate the number of graphene walls and the diameter distributions of as-grown CNTs. The chemical bonding states of as-grown CNT films were investigated using Raman spectroscopy.

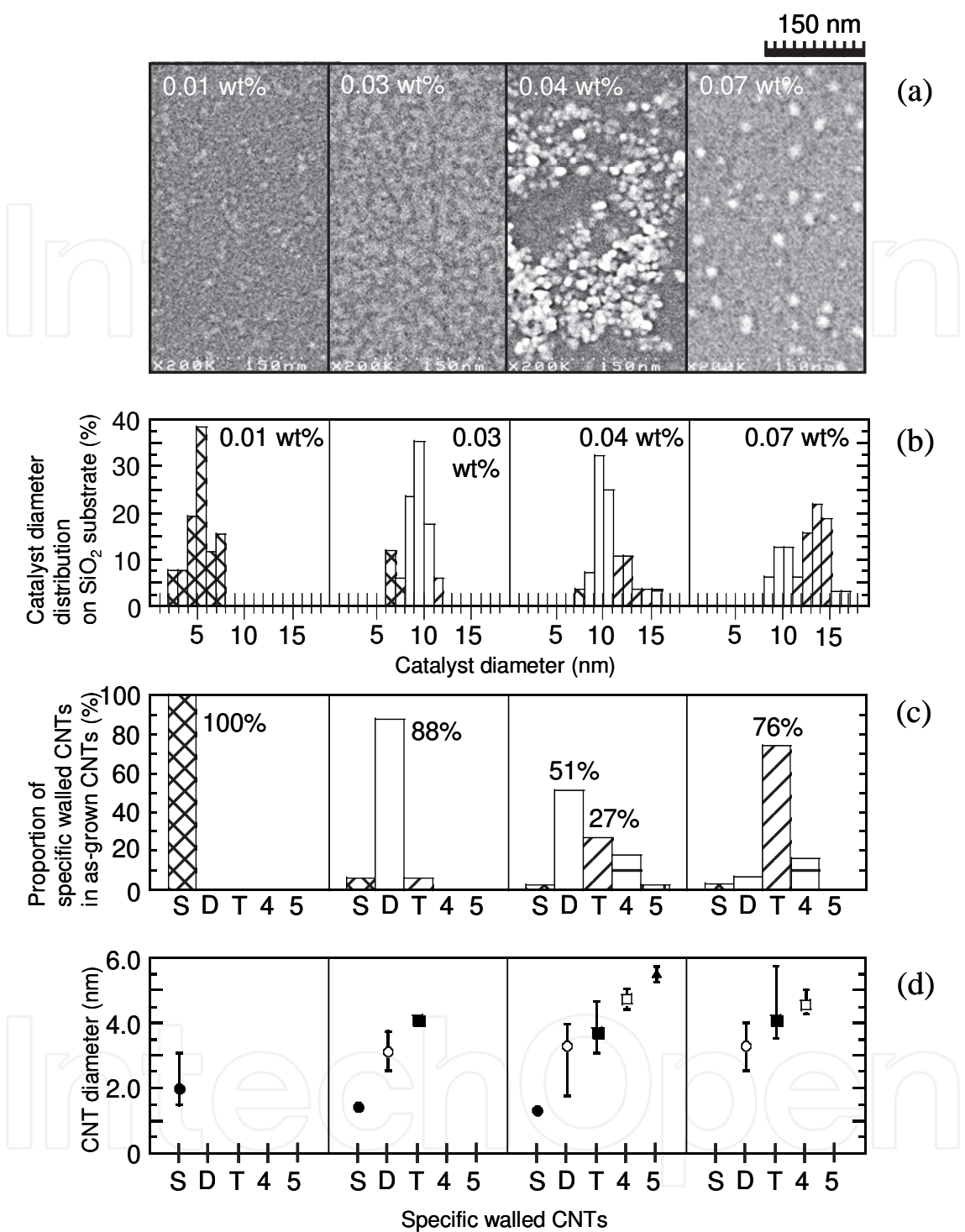


Fig. 1. Relationship between catalyst conditions on the eve of CNT growth and CNTs synthesized by RHCVD. (a) top-view SEM images of catalyst particles on quartz glass substrates dip-coated with 0.01, 0.03, 0.04, and 0.07 wt% solutions, (b) histograms of catalyst diameter distributions on the substrates, (c) histograms of specific walled CNTs, and (d) outer diameters of the specific walled CNTs.

It is important to understand the catalyst diameter distributions on substrates at the beginning of CNT growth. The CNT growth procedure explained above was executed until



the beginning of CNT growth. As soon as the substrate temperature reached 800°C, substrates were rapidly cooled down to room temperature without introducing ethanol vapor. The substrates obtained thus have similar appearances to the catalyst particles on the eve of CNT growth. Figure 1(a) shows top-view SEM images of the substrates on the eve of CNT growth, which were dip-coated with 0.01, 0.03, 0.04, and 0.07 wt% solutions and then reduced. The white regions are catalyst particles. Catalyst diameters were measured and are summarized in Fig. 1(b) in the histogram. Each histogram shows the sharp distribution within several nm. When a catalyst concentration in a dip solution is raised, catalyst diameters on a substrate increase. Therefore, catalyst diameters are able to be controlled by adjusting a concentration of catalyst in a dip solution.

Figure 2(a) shows an SEM image of the as-grown CNT film on the substrate that was dip-coated with a 0.01 wt% solution. The entire area of the substrate is covered with nonaligned CNTs. The CNTs gathered from the substrate shown in Fig. 2(a) were observed by TEM. The proportion of SWCNTs in the as-grown CNTs was 100%. Figure 3(a) shows TEM images of the as-grown SWCNTs. Figure 4(a) shows the Raman spectrum of the as-grown film shown in Fig. 2(a). The graphitic (G) band shape has a typical feature of SWCNTs, and the radial breathing mode (RBM) is clearly observed. Moreover, the disorder (D) band that arises from the disorder in the carbon arrangement is detected. The intensity ratio of the G band to the D band is 11 to 1.

Figure 2(b) shows an SEM image of the as-grown CNT film on the substrate that was dip-coated with a 0.03 wt% solution. The entire area of the substrate is covered with nonaligned CNTs. The CNTs gathered from the substrate shown in Fig. 2(b) were observed by TEM. The proportion of DWCNTs in the as-grown CNTs was 88%, and the remainder was composed of SWCNTs and TWCNTs. Figure 3(b) shows TEM images of the as-grown DWCNTs. Figure 4(b) shows the Raman spectrum of the as-grown film shown in Fig. 2(b). The D band is strengthened compared with that of the SWCNT film shown in Fig. 4(a). The detected RBM is attributed to the inner walls of the DWCNTs or SWCNTs.

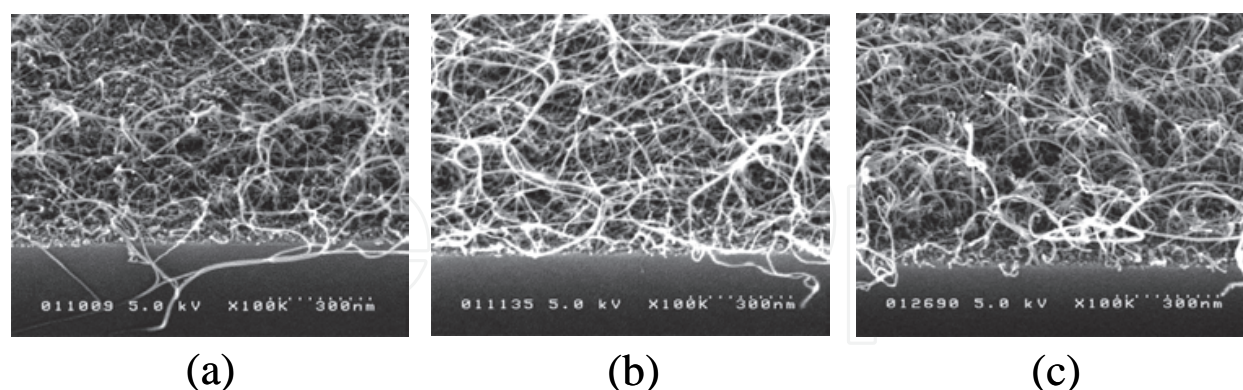


Fig. 2. SEM images of (a) SWCNT, (b) DWCNT, and (c) TWCNT films synthesized by RHCVD.

Figure 2(c) shows an SEM image of the as-grown CNT film on the substrate that was dip-coated with a 0.07 wt% solution. The entire area of the substrate is covered with nonaligned CNTs. The CNTs gathered from the substrate shown in Fig. 2(c) were observed by TEM. The proportion of TWCNTs in the as-grown CNTs was 76%, and the remainder was composed of DWCNTs and 4WCNTs. Figure 3(c) shows TEM images of the as-grown TWCNTs. Figure

4(c) shows the Raman spectrum of the as-grown film shown in Fig.2(c). The RBM is not detected. This result confirms that SWCNTs and DWCNTs with diameters smaller than 2.5nm are not included in this film. In addition, the G band becomes broader and the relative strength of the D band is higher. It is suggested that the amount of defects in CNTs increases as the number of graphene walls increases.

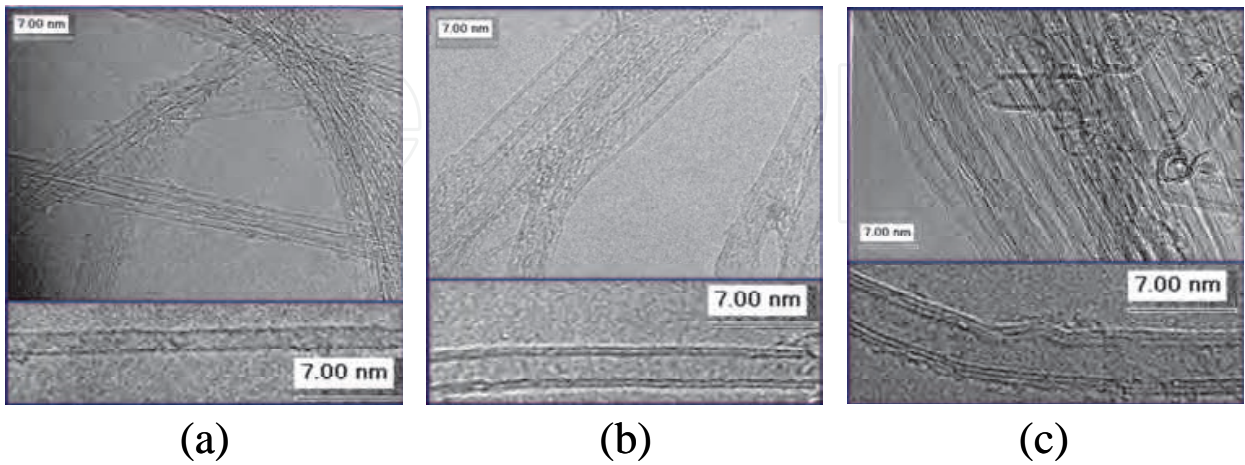


Fig. 3. TEM images of (a) SWCNTs, (b) DWCNTs, and (c) TWCNTs synthesized by RHCVD.

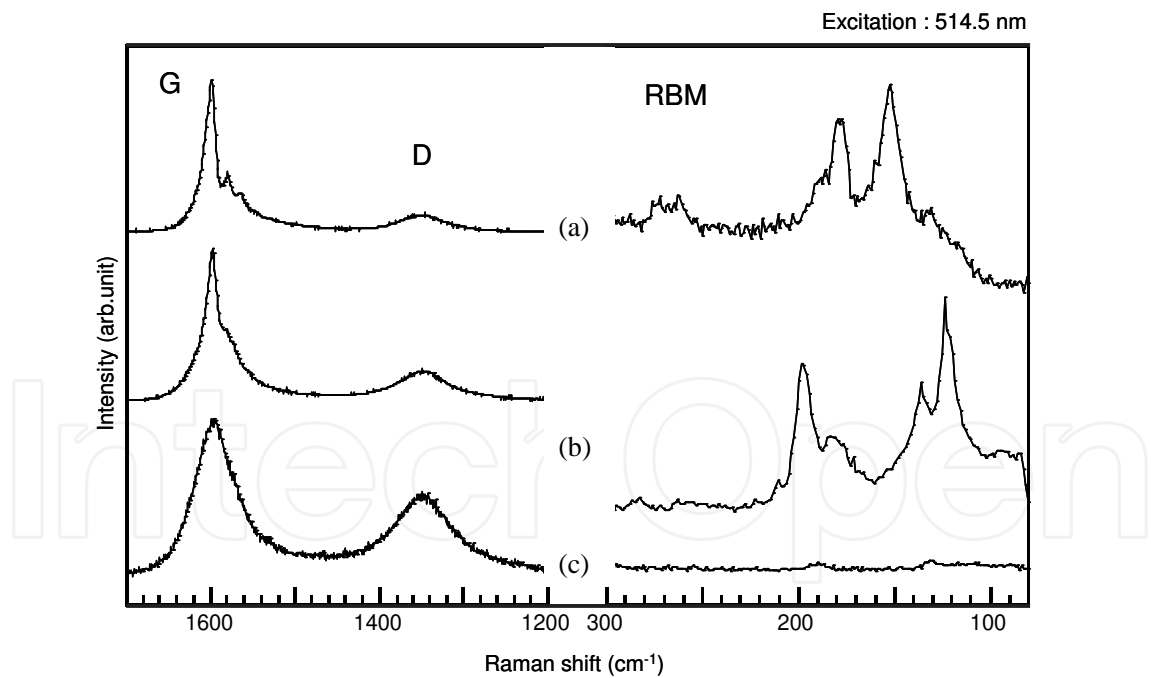


Fig. 4. Raman spectra of (a) SWCNT, (b) DWCNT, and (c) TWCNT films synthesized by RHCVD.

The discussion will now return to Fig. 1. CNTs were grown by RHCVD on each substrate with the catalyst diameter distribution shown in Fig. 1(b). The number of graphene walls was evaluated by TEM. The results are summarized in Fig. 1(c). Dominant CNTs are changed from SWCNTs and DWCNTs to TWCNTs as catalyst diameters increase. By

comparing Figs. 1(b) and 1(c) carefully, it seems that there are effective catalyst diameter ranges suitable for SW, DW, and TWCNT growth. SWCNTs grow when catalyst diameters are in the range of 2-8 nm. DWCNTs grow from catalysts with diameters of 8-11nm, and TWCNTs grow from catalysts with diameters of 11-15 nm. Figure 1(d) shows the outer diameters of CNTs measured by TEM. The number of graphene walls shows the tendency to increase as the outer diameters of CNTs increase. In addition, the outer diameters of CNTs are invariably smaller than the catalyst diameters.

A comparative study between RHCVD and conventional CVD (Murakami et al., 2004) was executed. The difference between the two processes is the heating rate used before the beginning of CNT growth. A dip solution with a concentration of 0.06wt% was prepared, and two quartz glass substrates were continuously dip-coated with the solution. Therefore, in the period before heating, the catalyst conditions of both substrates must be equivalent to each other. One substrate was heated using the conventional CVD procedure and the other substrate was heated using the RHCVD procedure. As soon as the temperature reached 800°C, both substrates were rapidly cooled down to room temperature without introducing ethanol vapor. Figure 5(a) shows histograms of the catalyst diameter distributions on both substrates measured by SEM. It is obvious that the catalyst diameter distribution obtained with the RHCVD procedure is comparatively narrow and has a sharp peak at 11-12 nm, while the distribution obtained with the conventional CVD procedure is broad and does not have a distinct peak.

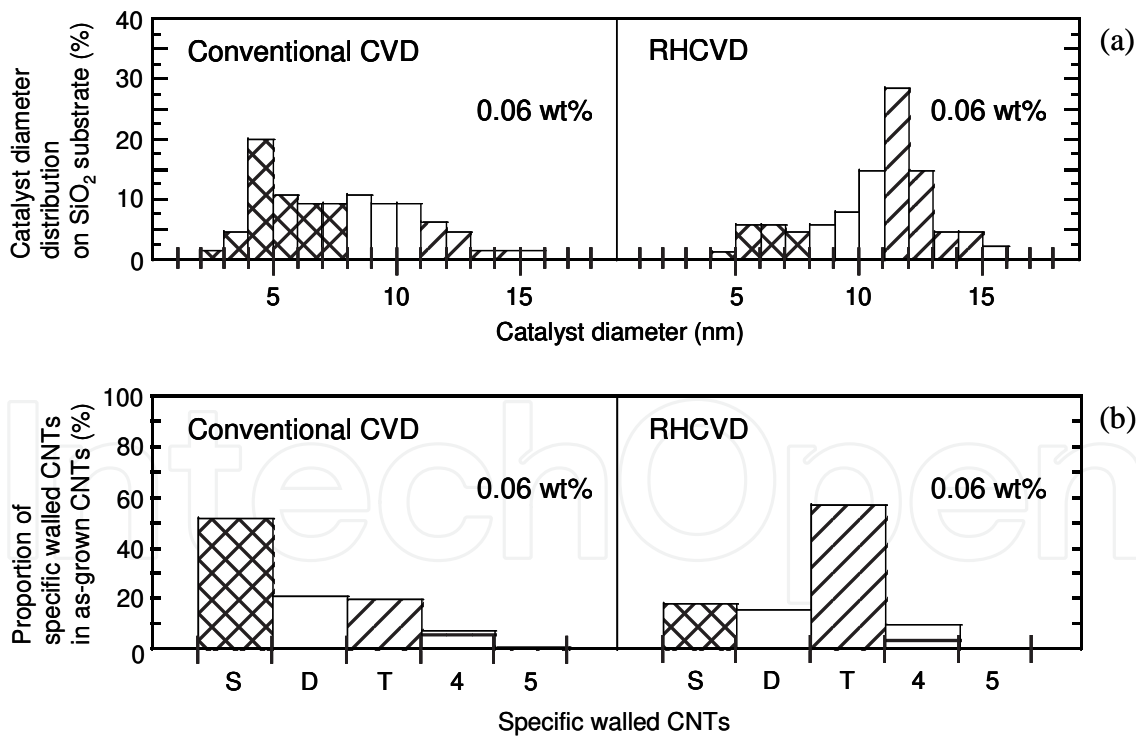


Fig. 5. Comparative study between RHCVD and conventional CVD. (a) histograms of the catalyst diameter distributions on quartz glass substrates dip-coated with a 0.06 wt% solution and heated up to 800°C, and (b) histograms of specific walled CNTs.

CNT growth was performed using substrates equal to those shown in Fig. 5(a). Figure 5(b) shows the results. In the case of conventional CVD, there are more SWCNTs than any other



CNTs. In the case of RHCVD, contrastingly, TWCNTs grow preferentially. From this comparative experiment, it has been confirmed that RHCVD is an effective process to selectively synthesize CNTs that consist of a specific number of graphene walls.

## 2.2 Selective growth of vertically aligned SWCNTs, DWCNTs, and TWCNTs by RHCVD

Quartz glass substrates were cleaned ultrasonically and then hydrophilically modified by UV irradiation in ambient atmosphere. A multicathode RF long-throw sputtering system was used for catalyst particle deposition.  $\text{Al}_2\text{O}_3$  particles as a non-catalyst were first deposited on the substrates with slightly larger diameter prior to metallic catalyst deposition. Secondly, both Co and Fe particles were deposited on the substrates as catalysts for SWCNT synthesis. Both Fe and Mo particles were deposited as catalysts for DWCNT and TWCNT syntheses. For a comparative study, MWCNT films were also synthesized with the catalysts of Fe particles. Catalyst diameters were adjusted by changing sputter time. The conversion film thicknesses of catalyst particles were calculated from sputter time. In this study, conversion film thicknesses were used as substitutes for catalyst diameters. After sputter deposition, the substrates for SW, DW, TW, and MWCNT syntheses were placed on a quartz glass holder in an RHCVD reactor simultaneously. The holder temperature was controlled with a thermocouple and a proportional-integral-derivative controller.

The RHCVD reactor was heated up and kept at an intermediate temperature in hydrogen atmosphere. Sputtered particles were reduced and they became metallic particles. The intermediate temperature is as low as the temperature at which catalyst particles scarcely aggregate and as high as the temperature at which the reduction reaction progresses sufficiently. Subsequently, the reactor was rapidly heated up to 800 °C in hydrogen atmosphere. As soon as the temperature reached 800 °C, ethanol vapor diluted with argon gas was introduced into the reactor. CNTs grew from the metallic catalyst particles on the substrates. During a CNT synthesis period of 1 h, the substrate temperature and total pressure were kept at 800 °C and 1.7 kPa, respectively.

The morphologies and lengths of the as-grown CNT films on substrates were observed by SEM. One hundred CNTs included in each film were observed by TEM in order to evaluate the number of graphene walls and the diameter distributions of the as-grown CNTs. In addition, the chemical bonding states of the as-grown SWCNTs were investigated by Raman spectroscopy. The photoluminescence (PL) properties of SWCNTs were also measured. PL gives the chirality distributions of semiconducting SWCNTs included in total SWCNTs.

SWCNT films are synthesized on the substrates on which both Co and Fe particles are deposited. When the total conversion film thickness of both particles is less than 0.40 nm and the Fe / Co thickness ratio ranges from 3 to 1/3, SWCNTs are preferentially synthesized. When coming off from this condition, MWCNTs are dominantly grown. The diameters of SWCNTs are proportional to the total film thickness of catalysts. Figure 6(a) shows an SEM image of the vertically aligned CNT film grown on a Co 0.15 nm / Fe 0.15 nm /  $\text{SiO}_2$  glass substrate. In this case, non-catalyst particles are not used. Figure 7(a) shows the TEM images of the CNTs extracted from the CNT film shown in Fig. 6(a). The CNTs are composed of SWCNTs (87 %), DWCNTs (10 %), and TWCNTs (3 %). The diameters of the SWCNTs are distributed from 1.2 to 4.0 nm, and the average diameter is 2.8 nm. Most SWCNTs form bundles, whereas some SWCNTs with relatively large diameters are naturally isolated.

Figure 8 shows the Raman spectra of the CNT film shown in Fig. 6(a). The radial breathing mode (RBM) appears clearly in Fig. 8(a). In Fig. 8(b), G band shape has a typical feature of SWCNTs and D band appears with a weak intensity. The intensity ratio of the G band to the D band is 16 to 1. The CNT film shown in Fig. 6(a) was removed from the substrate and then was ultrasonically dispersed in an aqueous solution of sodium dodecylbenzenesulfonate. After centrifugation, the upper solution was used for PL measurement. Figure 9 shows the PL properties of the SWCNTs synthesized by RHCVD and purified HiPco as a reference. These PL properties indicate the chirality distributions of small-diameter semiconducting SWCNTs included in both specimens. Although both have some common features, the most intense peaks are (7,5) and (8,3) in HiPco, while the most intense peak is (8,6) in the SWCNTs synthesized by RHCVD. From Raman and PL characterizations, it is clear that the as-grown SWCNTs synthesized by RHCVD have similar features to general SWCNTs synthesized by conventional CVD processes.

DWCNT films are synthesized on the substrates on which both Fe and Mo particles are deposited. When the total conversion film thickness of both particles ranges from 0.30 to 0.50 nm and the Fe / Mo thickness ratio ranges from 4 to 1, DWCNTs are preferentially synthesized. Figure 6(b) shows an SEM image of the vertically aligned CNT film grown on an Fe 0.30 nm / Mo 0.10 nm / Al<sub>2</sub>O<sub>3</sub> 5 nm / SiO<sub>2</sub> glass substrate. Figure 7(b) shows TEM images of the CNTs extracted from the CNT film. The CNTs shown in Fig. 7(b) are composed of DWCNTs (83 %) and TWCNTs (17 %). The outer diameters of the DWCNTs are distributed from 2.9 to 5.0 nm, and the average diameter is 4.1 nm.

TWCNT films are also synthesized on the substrates on which both Fe and Mo particles are deposited. When the total conversion film thickness of both particles ranges from 0.30 to 0.80 nm and the Fe / Mo thickness ratio ranges from 6 to 3, TWCNTs are preferentially synthesized. Figure 6(c) shows an SEM image of the vertically aligned CNT film grown on an Fe 0.25 nm / Mo 0.05 nm / Al<sub>2</sub>O<sub>3</sub> 5 nm / SiO<sub>2</sub> glass substrate. Figure 7(c) shows TEM images of the CNTs extracted from the CNT film. The CNTs shown in Fig. 7(c) are composed of DWCNTs (26 %), TWCNTs (62 %), and 4WCNTs (12 %). The outer diameters of the TWCNTs are distributed from 3.8 to 4.8 nm, and the average diameter is 4.4 nm.

MWCNT films are synthesized on the substrates on which only Fe particles are deposited. The diameters of MWCNTs are proportional to the conversion film thickness of Fe. Figure 6(d) shows an SEM image of the vertically aligned MWCNT film grown on an Fe 0.50 nm / Al<sub>2</sub>O<sub>3</sub> 5 nm / SiO<sub>2</sub> glass substrate. TEM observation revealed that the outer diameters of the MWCNTs are distributed from 5.3 to 9.5 nm, and the average diameter is 7.1 nm.

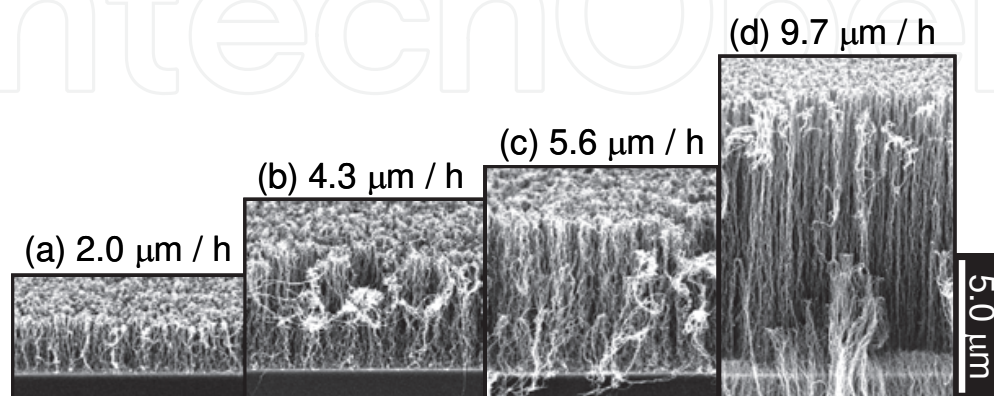


Fig. 6. SEM images of vertically aligned CNT films synthesized by RHCVD under optimal catalyst conditions for (a) SWCNTs, (b) DWCNTs, (c) TWCNTs, and (d) MWCNTs.

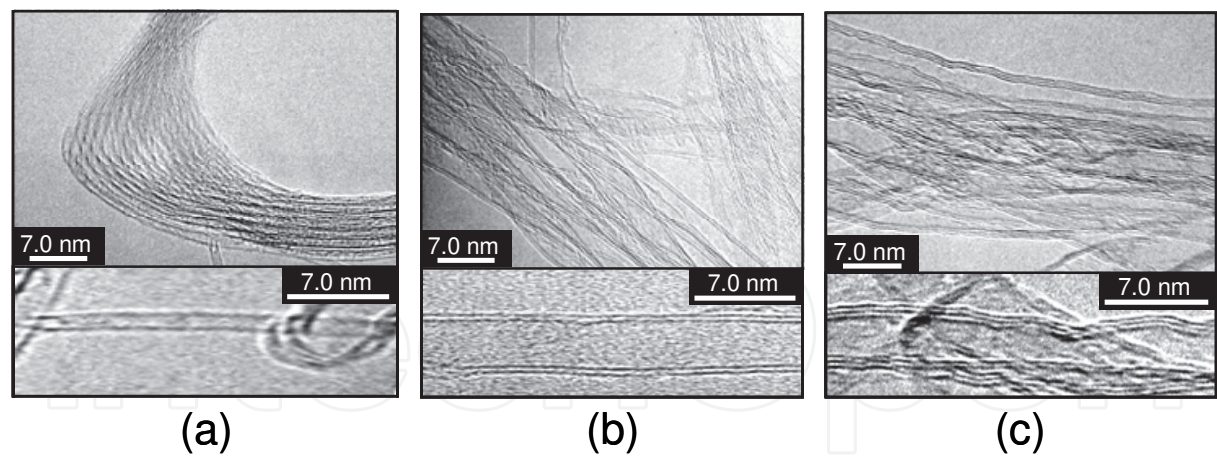


Fig. 7. TEM images of (a) SWCNTs, (b) DWCNTs, and (c) TWCNTs extracted from the CNT films shown in Figs. 6(a) - 6(c), respectively.

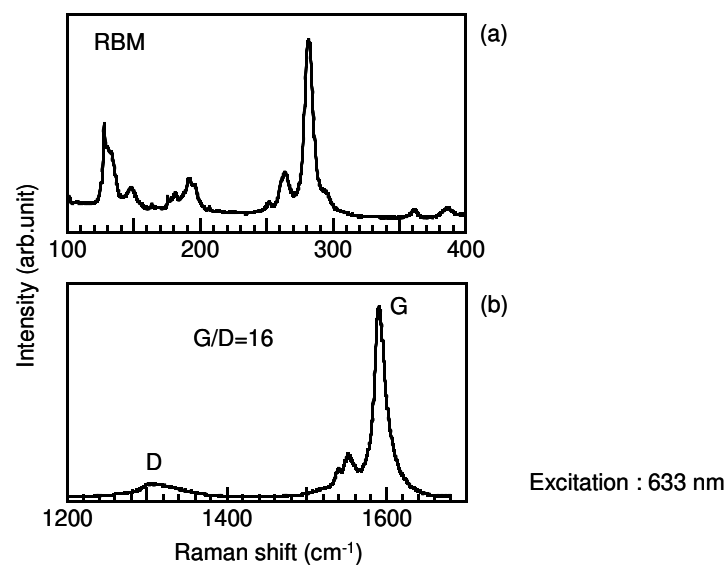


Fig. 8. Raman spectra of (a) RBM and (b) G-D regions of the CNT film shown in Fig. 6(a).

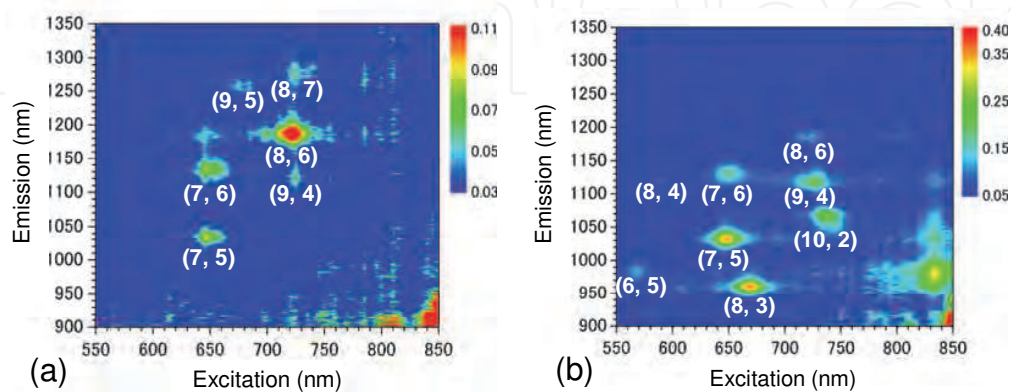


Fig. 9. PL properties of dispersed specimens of (a) the CNT film shown in Fig. 6(a) and (b) purified HiPco as a reference.



In this study, there are three important points concerning CNT growth, namely, the selection of graphene walls, vertical alignment, and lifetime of catalysts. These are sequentially discussed.

Figure 10 shows the proportions of specific walled CNTs / as-grown CNTs and the average outer diameters of the as-grown CNT films. The number of graphene walls of CNTs increases as the outer diameters of CNTs increase. Table 1 shows the total conversion film thicknesses and film thickness ratios of the main catalysts over the subcatalysts, which are used in order to synthesize the CNT films shown in Figs. 6(a)-6(d). Fe and Co are the main catalysts. Mo is considered to behave as the subcatalyst, which becomes an alloy with the main catalysts during heating, preventing the aggregation between the main catalyst particles. In the case of our long-throw sputtering, SWCNT films are not grown when both Fe/Mo and Co/Mo catalysts are used. From Fig. 10 and Table 1, it is clarified that the thickness ratio is important rather than the total thickness in achieving the selective growth of graphene walls. By alloying main catalyst particles with high melting-point metal particles, main catalyst particles are kept small and uniform in size.

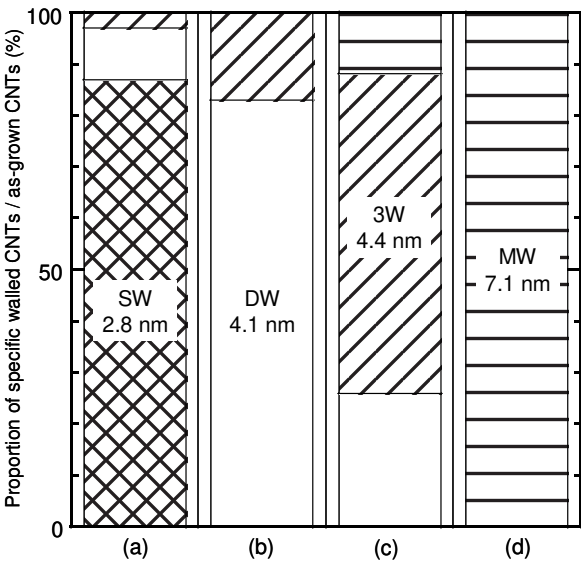


Fig. 10. Proportions of specific walled CNTs / as-grown CNTs and average outer diameters of the CNT films shown in Figs. 6(a) - 6(d). This result was obtained by TEM evaluation.

It is estimated from SEM observations that the population density of CNTs grown on a quartz glass substrate ranges from  $1.1 \times 10^9$  to  $7.1 \times 10^{10}$  bundles/cm<sup>2</sup>. The population density of CNTs on a substrate depends on the population density of non-catalyst particles adjusted by sputtering. When alloyed metallic particles are individually placed on each different non-catalyst particles and the population density of non-catalyst particles on a substrate is high enough, the alloyed metallic particles never aggregate and finally CNTs are able to vertically grow with the specific number of graphene walls. This phenomenon is similar to that observed in the case of a jam-packed train. In contrast, when the population density of alloyed catalyst particles without non-catalyst particles on a substrate is very low, CNTs do not grow vertically like the case of Section 2.1.

In Figs. 6(a)-6(d), as the outer diameters and the number of graphene walls of CNTs increase, CNTs grow longer. It is inferred that this result is due to the difference in lifetime between metallic catalysts. In short, the metallic catalysts become inactivated by intermediates decomposed from ethyl alcohol during a CNT growth period of 1 h. It needs



longer time to make larger metallic particles inactivated completely. It is considered that the larger the metallic catalyst diameter, the longer the catalyst lifetime.

	(a)	(b)	(c)	(d)
Selective growth	SWCNTs	DWCNTs	TWCNTs	MWCNTs
Total conversion film thickness	0.3	0.4	0.3	0.5
Film thickness ratio	Co/Fe=1	Fe/Mo=3	Fe/Mo=5	Fe only

Table 1. Total conversion film thicknesses and film thickness ratios of main catalysts over subcatalysts, which are used in order to synthesize the CNT films shown in Figs. 6(a) - 6(d).

2.3 Vertical growth of long CNTs by RHCVD

In order to make CNTs grow longer, it is necessary to delay the inactivation of metallic particles during a CNT growth period. Changing a non-catalyst from Al<sub>2</sub>O<sub>3</sub> to Al particles, and lowering a growth temperature from 800 °C to 650 °C are effective for delaying the inactivation of metallic catalysts. In Section 2.3, the vertically long TWCNT growth is explained with detailed data.

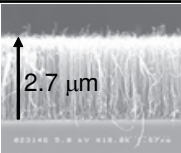
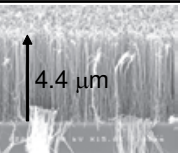
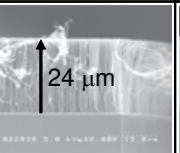
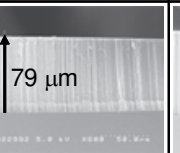
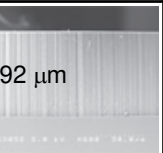
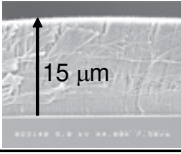
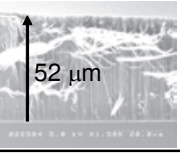
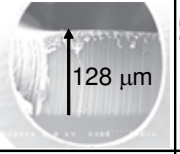
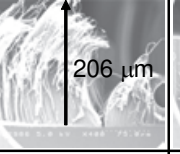
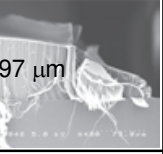
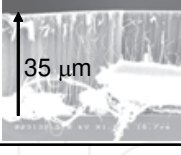
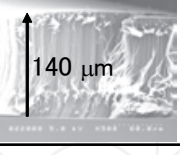
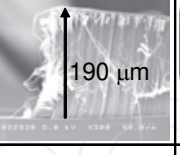
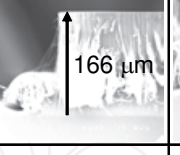
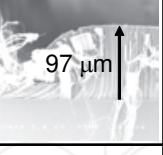
	800 °C	800 °C	750 °C	700 °C	650 °C
Center	 2.7 μm	 4.4 μm	 24 μm	 79 μm	 92 μm
Side	 15 μm	 52 μm	 128 μm	 206 μm	 97 μm
Corner	 35 μm	 140 μm	 190 μm	 166 μm	 97 μm
Co	1 nm	1 nm	1 nm	1 nm	1 nm
Fe	1 nm	1 nm	1 nm	1 nm	1 nm
Non-catalyst	Al <sub>2</sub> O <sub>3</sub> 5 nm	Al 5 nm	Al 5 nm	Al 5 nm	Al 5 nm

Fig. 11. SEM images of vertically aligned TWCNT films which locate at centers, sides, and corners of substrates, synthesized at various growth temperatures and catalyst conditions.

Figure 11 shows SEM images of CNTs grown from the alloy particles of Fe and Co on Al or Al<sub>2</sub>O<sub>3</sub> particles on quartz glass substrates. The growth time was 30 min. CNTs which grow at a center, a side, and a corner of each substate with a size of 20 mm<sup>2</sup> were observed by SEM. These CNTs were also confirmed to consist of mainly TWCNTs by TEM observation. In Fig.11, when comparing two kinds of CNTs synthesized at 800 °C, it is found that using Al particles instead of Al<sub>2</sub>O<sub>3</sub> can develop CNTs longer. Al is considered to react with intermediates easier than both Fe and Co. Al particles play a role of a getter catching

intermediates. In contrast, Because  $\text{Al}_2\text{O}_3$  itself is inert against intermediates, the lifetimes of Fe and Co become shorter and consequently CNTs grow shorter. Next, when comparing between CNTs synthesized at 800, 750, 700, and 650 °C, CNTs grow much longer at a lower temperature. This result attributes to delaying chemical reaction between metallic particles and intermediates at a lower temperature. Moreover, the difference of CNT length between a center, a side, and a corner in each substrate becomes smaller when lowering a growth temperature. This tendency is considered to the relatively larger distribution of Al particles in size since Al is low-melting point material. Lowering a growth temperature is also effective for synthesizing CNTs with uniform length in a wide area. Vertically long growth of SWCNTs and DWCNTs have been similarly accomplished though this chapter explained only TWCNTs.

### 3. Fabrication of transparent and anisotropically conductive plastic sheets by using CNTs

#### 3.1 Behavior of CNTs in an alternating electric field

An anisotropically conductive CNTs sheet is fabricated by using dielectrophoresis phenomena. In general, when particles are placed in an alternating electric field, polarization is created inside the particles. As a result, two kinds of forces generated inside particles depending on an alternating frequency. Under a relatively low frequency, particles move to the region of higher electric field. This is called positive dielectrophoresis. In contrast, when non-conductive particles are under a relatively high frequency, non-conductive particles move to the region of lower electric field. This is called negative dielectrophoresis. Positive dielectrophoresis phenomenon is utilized to fabricate anisotropically conductive CNT sheets. At first, the distribution of electric field intensity was calculated by finite element method. Figure 12 shows the cross-sectional distribution of electric field intensity between both electrodes. The distance between both electrodes is 100  $\mu\text{m}$  and the medium is pure water. The electric field intensity becomes much stronger near both electrodes, especially, at the edges of electrodes, the electric field intensity is maximum. On the other hand, in the intermediate region between both electrodes, the electric field intensity is minimum. Therefore, when particles are influenced by positive dielectrophoresis, the particles move quickly toward both electrodes.

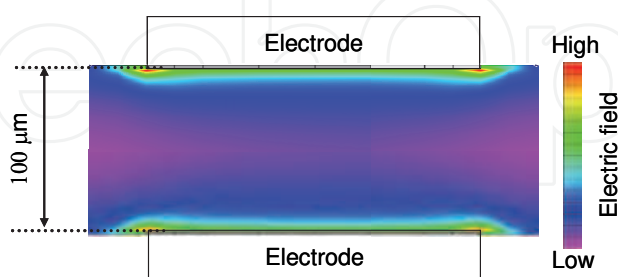


Fig. 12. Cross-sectional distribution of electric field intensity between both electrodes.

In order to understand the behavior of CNTs in dielectrophoresis, a basic experiment was performed. The circuit as illustrated in Fig 12 was prepared. ITO films were deposited on a pair of glass substrates as both electrodes, because particles could be observed to move during dielectrophoresis with a microscope. SWCNTs were ultrasonically treated in a 5 mol/L-nitric acid solution for cutting the lengths of CNTs. Treated CNTs were dispersed in

pure water with a concentration of 1 mg/mL, and the dispersion liquid was dropped on the circuit. When an AC voltage of 4 Vp-p was applied with a frequency of 100 kHz, SWCNTs were observed to move quickly to both surfaces of ITO electrodes. Figure 13 shows an SEM image of an area near one electrode in a few seconds just after starting to apply an AC voltage. In Fig 13, first reached SWCNTs are observed to align perpendicularly to the surface of the electrode. Secondly reached SWCNTs connect to the edges of first reached SWCNTs, and Tertiarily reached SWCNTs connect to the edges of secondarily reached SWCNTs. Because CNTs have such a fiber-like shape, polarization is created between both edges and center of CNTs. As a result, CNTs always move and align as shown Fig 13. After applying an AC voltage between both electrodes, CNTs finally connect between both electrodes and an electrical circuit is closed.

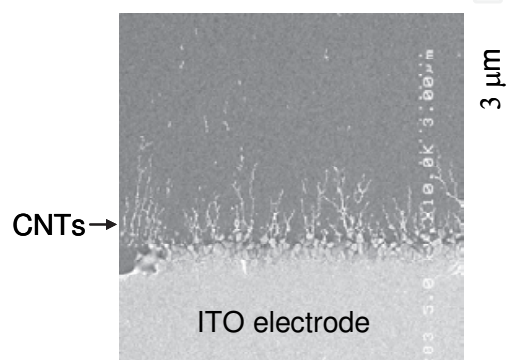


Fig. 13. SEM image of CNTs aligned perpendicularly at an ITO electrode in the early stage of positive dielectrophoresis.

### 3.2 Transparent and anisotropically conductive plastic sheets containing CNTs

By utilizing this fundamental and interesting behavior of CNTs in dielectrophoresis, an anisotropically conductive CNT sheet can be fabricated. CNTs are treated in a 5 mol/L-nitric acid solution for cutting the lengths of CNTs, rinsed with pure water and ethanol, and then dispersed in a polymer medium by ultrasonic homogenizer for 20 min. Low viscosity acrylic acid resin R-604 is used as a polymer medium. The viscosity is 500 cP and the contraction percentage is approximately 7 %. The molecular structure of R-604 is illustrated in Fig 14. A pair of flat glass substrates are prepared, and Au films with a thickness of 50 nm are deposited on one side of each substrate as electrodes. A pair of Au electrodes are faced and fixed with a space of 100 μm. The space is easily adjusted with spacers. The polymer medium in which CNTs are dispersed is introduced into the space between the electrodes. When applying an alternating voltage of 20 Vp-p with a frequency of 1 kHz to 100 kHz, CNTs move toward the electrodes, align perpendicularly to the surfaces of electrodes, finally connect between both electrodes in the polymer medium. Positive dielectrophoresis takes place same as the case of water medium. During positive dielectrophoresis, the circuit current is continuously monitored. When the current rapidly increases, the circuit is irradiated with UV light while applying the voltage. After polymer becomes solid, irradiating with UV light and applying the voltage are finished. Molded plastic sheet is easily removed from a pair of substrates, because Au electrode films also play a role of mold lubricant. If necessary, after demolding, both sides of the plastic sheet are coated with transparent material such as ITO, ZnO and so on. This consecutive procedure is shown in Fig 15.

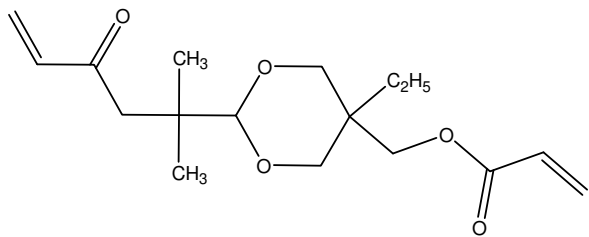


Fig. 14. Molecular structure of acrylic acid resin R-604.

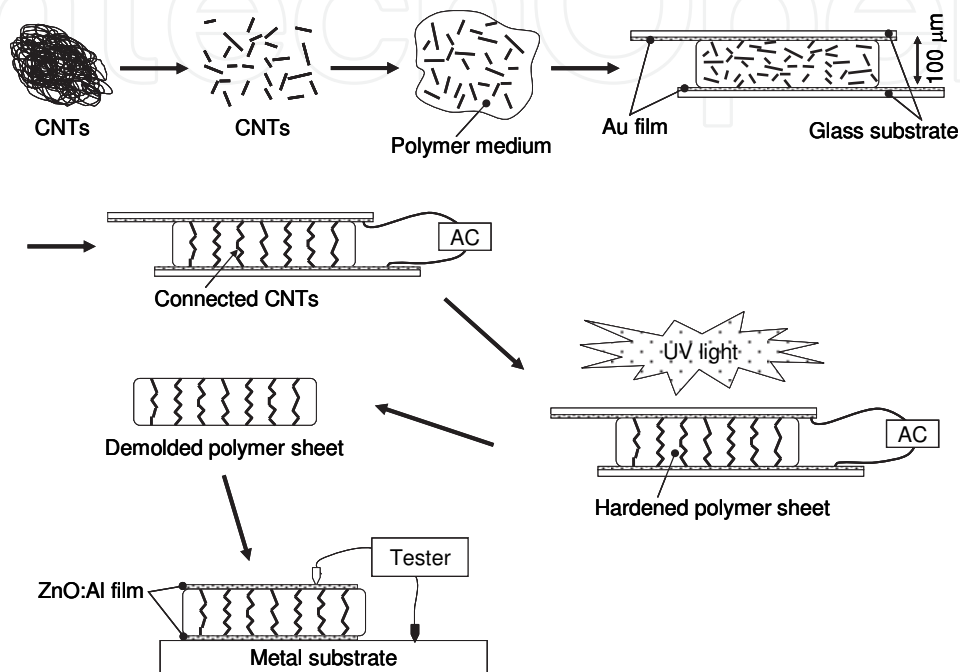


Fig. 15. Procedure for fabricating a transparent and anisotropically conductive plastic sheet containing CNTs.

Figure 16 shows typical appearances of a plastic sheet conatining CNTs and an original plastic sheet without CNTs. Because CNTs are aligned perpendicularly to a surface of a plastic sheet, a CNT-containing plastic sheet is completely transparent in visible light, as shown in Fig 16(a).

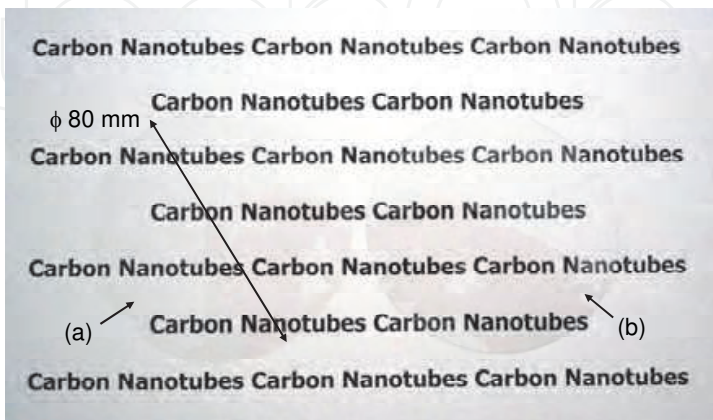


Fig. 16. Appearances of (a) an transparent and anisotropically conductive plastic sheet conatining CNTs, and (b) an original plastic sheet without CNTs.



For comparative study, SWCNTs, MWCNTs, and TWCNTs were used in order to fabricate conductive plastic sheets. Table 2 shows providers, the number of graphene walls, approximate average diameters and lengths of CNTs. SWCNTs were cut by nitric acid treatment. MWCNTs were purified by alkaline and then cut by nitric acid treatment. On the other hand, as mentioned in Section 2.3, a vertically long TWCNT film with 90  $\mu\text{m}$  long was synthesized on a quartz glass substrate, and then was scratched from the glass substrate. The TWCNTs were used without nitric acid treatment. By using these CNT sources at conditions of 1 kHz and 20Vp-p, conductive plastic sheets were fabricated. The results are summarized in Table 3. Electrical resistivity was measured two times, before demolded, and after demolded and coated with ZnO:Al film. All four plastic sheets have conductivity in perpendicular direction, in contrast, high resistivity in in-plane direction. This indicates that CNTs are completely oriented and connected perpendicularly in molded plastic sheets. The lengths of TWCNTs are much longer than the other CNTs. Therefore, the number of connecting points between each CNT in a sheet is considered less than the other CNTs. This is the main reason why the sheet containing TWCNTs have much lower resistivity than the other sheets containing SWCNTs and MWCNTs. Figure 17 shows transmittance and reflectance spectra of anisotropically conductive plastic sheets containing three kinds of CNTs with different concentrations, and an insulating plastic sheet without CNTs as a reference. These anisotropically conductive plastic sheets give high enough transparency through the visible region.

CNTs	The number of graphene wall	CNT diameter (nm)	CNT length ( $\mu\text{m}$ )
SWCNTs (CNI, HiPco)	1	about 1	0.2 After nitric acid treatment
MWCNTs (Meijo Nano Carbon)	about 20	about 20	0.2 After nitric acid treatment
TWCNTs (Nikon)	Mainly 3	3 ~ 6	90 As-grown

Table 2. The number of graphene walls, diameters, and lengths of SWCNTs, TWCNTs, and MWCNTs used for fabricating transparent and anisotropically conductive plastic sheets.

CNTs	CNT content (wt%)	Sheet thickness ( $\mu\text{m}$ )	Sheet transmittance @ 500 nm (%)	Resistivity ( $\Omega$ )		
				Before demolding		After demolding
				perpendicular	parallel	perpendicular
SWCNTs (CNI, HiPco)	0.01	~100	90.3	920	$>10^{14}$	867
MWCNTs (Meijo Nano Carbon)	0.01	~100	91.0	1,500	$>10^{14}$	900,000
TWCNTs (Nikon)	0.01	~100	81.9	58	$>10^{14}$	58
TWCNTs (Nikon)	0.005	~100	86.9	104	$>10^{14}$	111

Table 3. Transmittances and electrical resistivities of transparent and anisotropically conductive plastic sheets containing SWCNTs, TWCNTs, and MWCNTs.

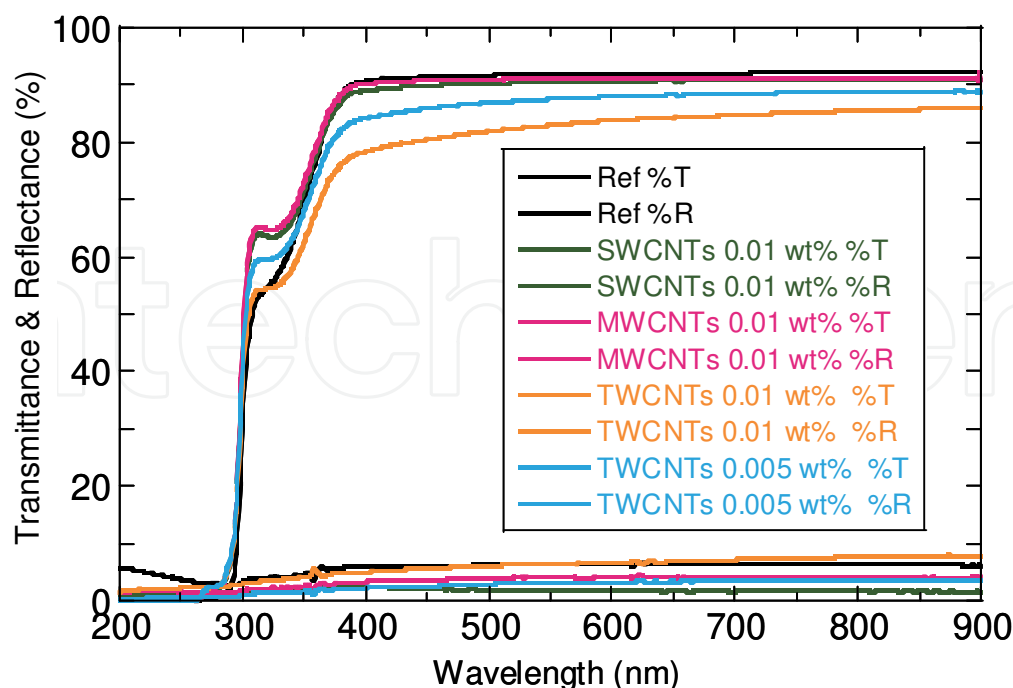


Fig. 17. Transmittance and reflectance spectra of transparent and anisotropically conductive plastic sheets containing SWCNTs, TWCNTs, and MWCNTs, and an insulating plastic sheet without CNTs.

#### 4. Optical filters by using CNT forests

A vertically aligned CNT film, in other words, a CNT forest was synthesized on a quartz glass substrate by RHCVD as stated in Section 2.3. Figure 18 shows an appearance and a cross-sectional SEM image of a typical CNT forest. In Fig.18, the CNT forest is observed to be black enough without reflection, and identified to grow vertically on a substrate with a high population density. The absolute transmittance and reflectance of the CNT forest are  $T=0.0002\%$  (optical density,  $OD = 5.7$ ) and  $R=0.0018\%$  (at an incident angle of  $5^\circ$ ) at  $193.4\text{ nm}$  of ArF laser wavelength, measured with Cary 5 (Varian) and U-4000 (Shimadzu) respectively. The reflectance of the CNT forest is less than  $0.002\%$  at an incident angle of  $5^\circ$  in the wide wavelength range from ultraviolet to infrared. In addition, the reflectance of the CNT forest was also measured under wide incident angles of  $10$  to  $80^\circ$  at  $193.4\text{ nm}$  with VUV-VASE (J.A.Woollam), as shown in Fig 19. The reflectance of the CNT forest is less than  $0.01\%$  up to incident angles of  $75^\circ$ , and less than  $0.35\%$  up to an incident angles of  $80^\circ$ . Extremely low-reflection feature is achieved at such a wide incident angle range. This CNT forest performs as an anti-reflective black filter in a wide incident angle range and wide wavelength range. The ArF laser marathon test of the CNT forest shown in Fig.18 was performed. The CNT forest was irradiated with ArF laser up to doses of  $7.5 \times 10^8\text{ mJ/cm}^2$  under nitrogen gas purge environment. Figures 20 & 21 show the OD value and reflectance as a function of the dose of ArF laser. The OD value merely decreases from  $5.7$  to  $5.5$  during the marathon test. This degradation can be small enough and negligible. The reflectance is maintained less than  $0.002\%$  through the test. This results have proven practical stability of the CNT forest as an anti-reflective black filter for ArF laser.

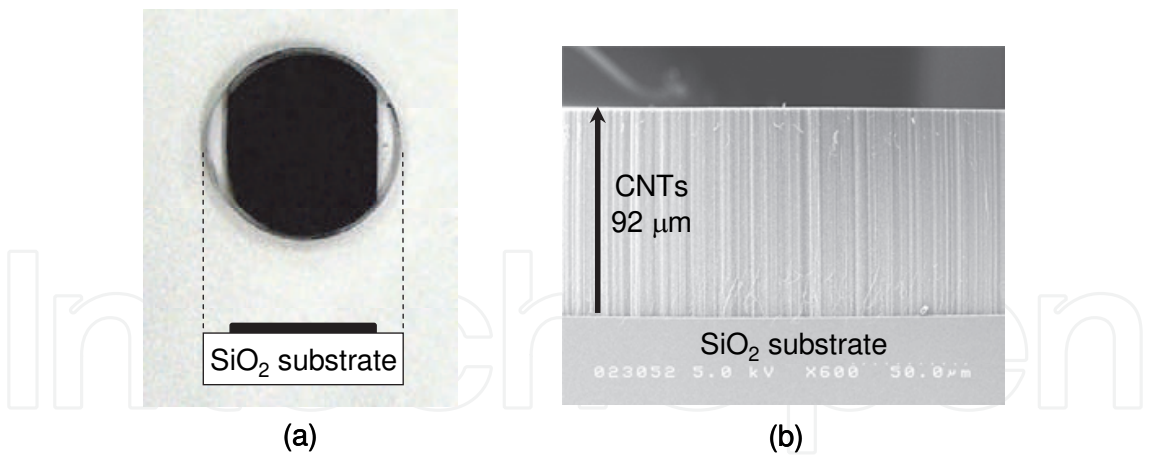


Fig. 18. (a) an appearance and (b) a cross-sectional SEM image of a typical CNT forest.

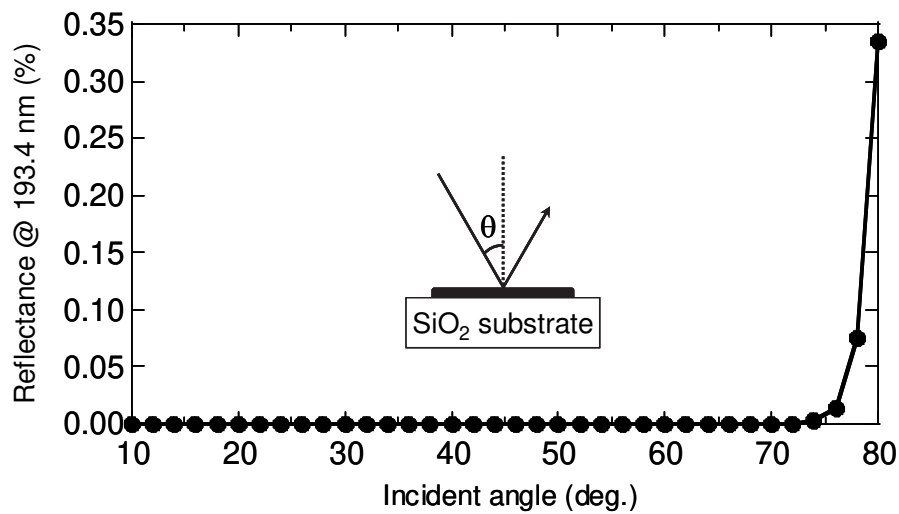


Fig. 19. Incident angle dependence of the reflectance at 193.4 nm of a CNT forest.

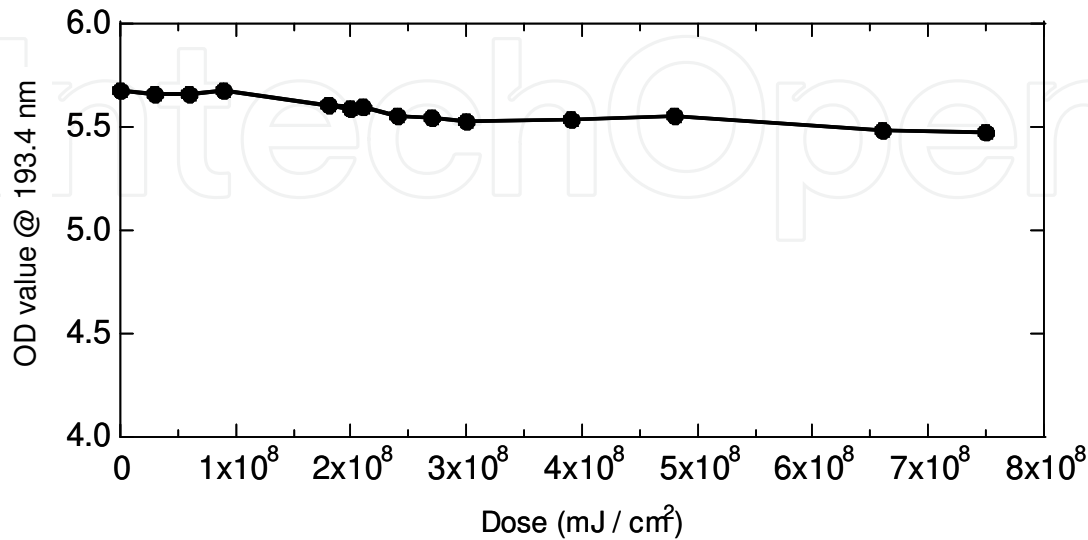


Fig. 20. OD value changes of a CNT forest duirng long-time ArF laser irradiation.

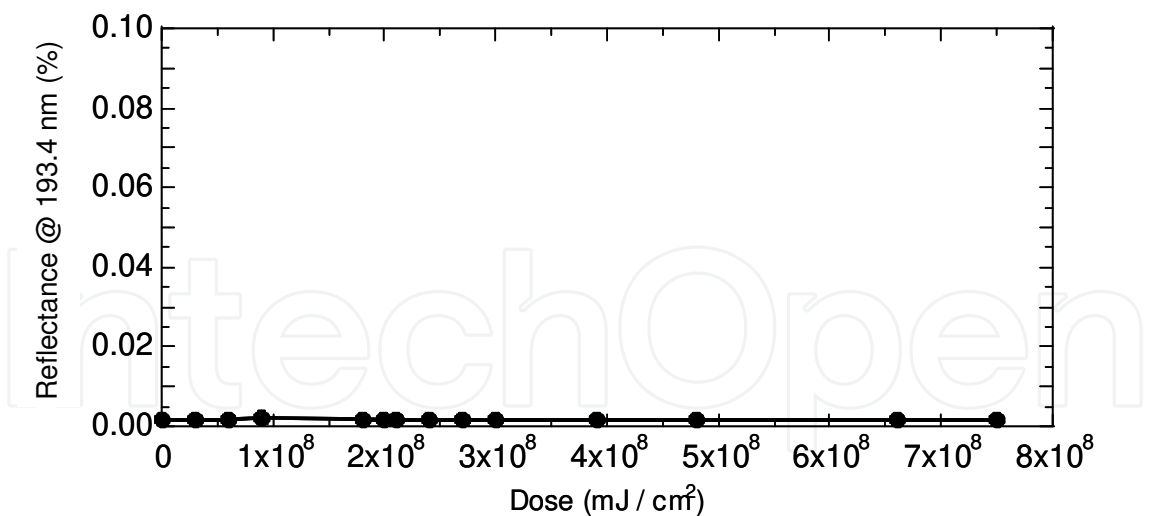


Fig. 21. Reflectance changes of a CNT forest duirng long-time ArF laser irradiation.

Detailed investigation regarding to the thickness of CNT forests revealed that CNT forests more than 10  $\mu\text{m}$  long on quartz glass substrates perform as anti-reflective black filters. On the other hand, CNT forests of a few microns long are useful for ND filters. By changing catalyst diameters, a CNT growth time, and a CNT growth temperature, the OD value is adjusted sequentially. Figure 22 shows top-view appearances, OD values, and reflectances at 193.4 nm of CNT forests deposited by different growth conditions. In addition, the easier way to adjust an OD vaule of a ND filter is shown in Fig 23. Stacking of a metallic Cr film and a CNT forest of a few microns long performs as an anti-reflective ND filter. First, a Cr film is deposited on a quartz glass substrate, secondarily, a CNT forest is grown on the Cr film. The optical density of the ND filter is adjusted by the thickness of the Cr film. The CNT forest plays a role of anti-reflection. A CNT forest is capable of a unique optical filter.

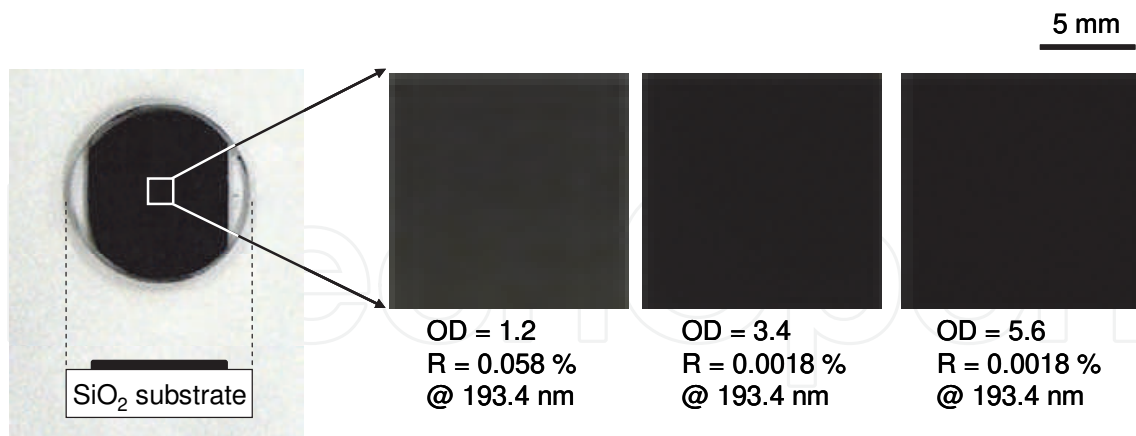


Fig. 22. Colors, OD values and reflectances at 193.4 nm of CNT forests with various lengths.

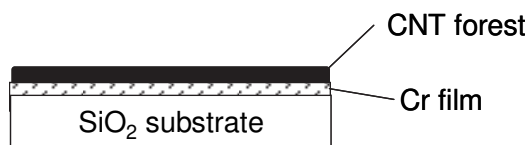


Fig. 23. Illustration of stacking of a Cr film and a CNT forest for an anti-reflective ND filter.



## 5. Conclusions

RHCVD is a newly developed process that enables the maintenance of narrow catalyst diameter distributions until CNTs start growing, and the syntheses of SWCNT (SWCNT / as-grown CNT ratio of 100%), DWCNT (DWCNT / as-grown CNT ratio of 88%), and TWCNT (TWCNT / as-grown CNT ratio of 76%) films by changing catalyst diameters. It is clarified that catalyst diameters have a close relationship to CNT diameters and the number of graphene walls of CNTs.

The syntheses of vertically aligned SWCNT, DWCNT, and TWCNT films have been achieved by a combination of RHCVD and the particle-arranged substrates where alloyed catalyst particles are deposited on non-catalyst particles. The diameters of non-catalyst particles must be slightly larger than those of catalyst particles. Because each catalyst particle is located on each non-catalyst particle, a catalyst particle is not able to aggregate with a nearest catalyst particle on another non-catalyst particle during pre-heating process. Therefore, CNTs are able to grow vertically on a substrate with a high population density.

Metallic catalysts become inactivated by intermediates decomposed from ethyl alcohol as a carbon source during a CNT growth period. In order to make CNTs grow longer, it is necessary to delay the inactivation of metallic particles during a CNT growth period. By using Al particles as a non-catalyst, and lowering a growth temperature up to 650 °C, vertically long SWCNT, DWCNTs, and TWCNT growth has been accomplished. Al particles play a role of a getter catching intermediates. Lowering a growth temperature delays chemical reaction between metallic particles and intermediates.

The new method to fabricate a transparent and conductive plastic sheet with CNTs has been developed. CNTs are dispersed in a polymer medium. While casting a plastic sheet with the polymer medium, positive dielectrophoresis of CNTs is executed in the polymer medium. CNTs align perpendicularly to both surfaces of the sheet, and finally connect between both surfaces of the sheet. By irradiating with UV light to solidify the sheet, an anisotropically conductive CNT sheet is fabricated. A remarkable feature of this transparent sheet is its conductivity in perpendicular direction and high resistivity in-plane direction.

By using a CNT forest, a unique optical filter has been developed. A CNT forest more than 10 µm long on a quartz glass substrate performs as an anti-reflective black filter. The reflectance of a CNT black filter is nearly zero in the wide wavelength range from ultraviolet to infrared and the wide incident angles from 0 deg to 75 deg. A CNT black filter has been proven to be capable of ArF laser applications. On the other hand, a CNT forest of a few microns long performs as an anti-reflective ND filter by stacking of a metallic Cr film and a CNT forest.

## 6. References

- Dan B., Irvin G.C., & Pasquali M. (2009). Continuous and Scalable Fabrication of Transparent Conducting Carbon Nanotube Films. *ACS Nano*, Vol.3, No.4, (April 2009), pp. 835-843
- Hata K., Futaba D. N., Mizuno K., Namai T., Yumura M., & Iijima S. (2004). Water-Assisted Highly Efficient Synthesis of Impurity-Free Single-Walled Carbon Nanotubes. *Science*, Vol. 306, No. 5700, (November 2004), pp. 1362-1364

- Hecht D.S., Thomas D., Hu L., Ladous C., Lam T., Park Y., Irvin G., & Drzaic P. (2009). Carbon-nanotube film on plastic as transparent electrode for resistive touch screens. *Journal of the Society for Information Display*, Vol. 17, No. 11, (November 2009), pp. 941-946, ISSN 10710922
- Hiramatsu M., Nagao H., Taniguchi M., Amano H., Ando Y., & Hori M. (2005). High-Rate Growth of Films of Dense, Aligned Double-Walled Carbon Nanotubes Using Microwave Plasma-Enhanced Chemical Vapor Deposition. *Japanese Journal Applied Physics*, Vol. 44, No. 22, (May 2005), pp. L 693 – L 695
- Murakami Y., Chiashi S., Miyauchi Y., Hu M., Ogura M., Okubo T., & Maruyama S. (2004). Growth of Vertically Aligned Single-Walled Carbon Nanotube Films on Quartz Substrates and Their Optical Anisotropy. *Chemical Physics Letters*, Vol. 385, No. 3-4 (February 2004), pp. 298-303
- Muramatsu H., Hayashi T., Kim Y. A., Endo M., Terrones M., & Dresselhaus M. S. (2005). Growth of Double-Walled Carbon Nanotubes Using a Conditioning Catalyst. *Journal of Nanoscience and Nanotechnology*, Vol. 5, No. 3, (March 2005), pp. 404-408, ISSN 15334880
- Nikolaev P., Bronikowski M. J., Bradley R. K., Rohmund F., Colbert D. T., Smith K. A., & Smalley R. E. (1999). Gas-Phase Catalytic Growth of Single-Walled Carbon Nanotubes from Carbon Monoxide. *Chemical Physics Letters*, Vol. 313, No. 1-2, (November 1999), pp. 91-97
- Ramesh P., Okazaki T., Sugai T., Kimura J., Kishi N., Sato K., Ozeki Y., & Shinohara H. (2006). Purification and Characterization of Double-Wall Carbon Nanotubes Synthesized by Catalytic Chemical Vapor Deposition on Mesoporous Silica. *Chemical Physics Letters*, Vol. 418, No. 4-6, (February 2006), pp. 408-412
- Taki Y., Shinohara K., Kikuchi M., & Tanaka A. (2008). Selective Growth of Single-, Double-, and Triple-Walled Carbon Nanotubes through Precise Control of Catalyst Diameter by Radiation-Heated Chemical Vapor Deposition. *Japanese Journal Applied Physics*, Vol. 47, No. 1, (January 2008), pp. 725 – 729
- Taki Y., Kikuchi M., Shinohara K., & Tanaka A. (2008). Selective Growth of Vertically Aligned Single-, Double-, and Triple-Walled Carbon Nanotubes by Radiation-Heated Chemical Vapor Deposition. *Japanese Journal Applied Physics*, Vol. 47, No. 1, (January 2008), pp. 721 – 724
- Wu Z., Chen Z., Du X., Logan J.M., Sippel J., Nikolou M., Kamaras K., Reynolds J.R., Tanner D.B., Hebard A.F., Rinzler A.G. (2004). Transparent, conductive carbon nanotube films. *Science*, Vol. 305, No. 5688, (August 2004), pp. 1273-1276, ISSN 00368075
- Yamada T., Namai T., Hata K., Futaba D. N., Mizuno K., Fan J., Yudasaka M., Yumura M., & Iijima S. (2006). Size-Selective Growth of Double-Walled Carbon Nanotube Forests from Engineered Iron Catalysts. *Nature Nanotechnology*, Vol. 1, (November 2006), pp. 131-136

Zhong G., Iwasaki T., Honda K., Furukawa Y., Ohdomari I., & Kwarada H. (2005). Low Temperature Synthesis of Extremely Dense and Vertically Aligned Single-Walled Carbon Nanotubes. *Japanese Journal Applied Physics*, Vol. 44, No. 4A, (April 2005), pp. 1558 - 1561

IntechOpen

IntechOpen



## **Carbon Nanotubes - Synthesis, Characterization, Applications**

Edited by Dr. Siva Yellampalli

ISBN 978-953-307-497-9

Hard cover, 514 pages

**Publisher** InTech

**Published online** 20, July, 2011

**Published in print edition** July, 2011

Carbon nanotubes are one of the most intriguing new materials with extraordinary properties being discovered in the last decade. The unique structure of carbon nanotubes provides nanotubes with extraordinary mechanical and electrical properties. The outstanding properties that these materials possess have opened new interesting researches areas in nanoscience and nanotechnology. Although nanotubes are very promising in a wide variety of fields, application of individual nanotubes for large scale production has been limited. The main roadblocks, which hinder its use, are limited understanding of its synthesis and electrical properties which lead to difficulty in structure control, existence of impurities, and poor processability. This book makes an attempt to provide indepth study and analysis of various synthesis methods, processing techniques and characterization of carbon nanotubes that will lead to the increased applications of carbon nanotubes.

### **How to reference**

In order to correctly reference this scholarly work, feel free to copy and paste the following:

Yusuke Taki, Makiko Kikuchi, Kiyooki Shinohara, Yosuke Inokuchi and Youhei Takahashi (2011). Selective Growth of Carbon Nanotubes and Their Application to Transparent Conductive Plastic Sheets and Optical Filters, Carbon Nanotubes - Synthesis, Characterization, Applications, Dr. Siva Yellampalli (Ed.), ISBN: 978-953-307-497-9, InTech, Available from: <http://www.intechopen.com/books/carbon-nanotubes-synthesis-characterization-applications/selective-growth-of-carbon-nanotubes-and-their-application-to-transparent-conductive-plastic-sheets->

**INTECH**  
open science | open minds

### **InTech Europe**

University Campus STeP Ri  
Slavka Krautzeka 83/A  
51000 Rijeka, Croatia  
Phone: +385 (51) 770 447  
Fax: +385 (51) 686 166  
[www.intechopen.com](http://www.intechopen.com)

### **InTech China**

Unit 405, Office Block, Hotel Equatorial Shanghai  
No.65, Yan An Road (West), Shanghai, 200040, China  
中国上海市延安西路65号上海国际贵都大饭店办公楼405单元  
Phone: +86-21-62489820  
Fax: +86-21-62489821



© 2011 The Author(s). Licensee IntechOpen. This chapter is distributed under the terms of the [Creative Commons Attribution-NonCommercial-ShareAlike-3.0 License](https://creativecommons.org/licenses/by-nc-sa/3.0/), which permits use, distribution and reproduction for non-commercial purposes, provided the original is properly cited and derivative works building on this content are distributed under the same license.

IntechOpen

IntechOpen